Morphological study of a chiral polymer network in a nematic liquid crystal from a concentration gradient

Michel Mitov, Alain Boudet, Pierre Sopena, Pierre Sixou

Accepted version published in: *Liquid Crystals*, **23**, 903-910 (1997)

Morphological study of a chiral polymer network in a nematic liquid crystal from a concentration gradient

Michel Mitov*, Alain Boudet, Pierre Sopéna

CEMES (CNRS UPR 8011), BP 4347, F-31055 Toulouse Cedex 4, France

and Pierre Sixou

LPMC (CNRS UMR 6622), Parc Valrose, F-06108 Nice Cedex 2, France

Article history: Received 27 June 1997. Accepted 29 July 1997.

https://www.tandfonline.com/doi/abs/10.1080/026782997207849

A contact preparation is made between a cholesteric photocrosslinkable material and a standard nematic liquid crystal. The concentration and the anisotropy progressively and homogeneously vary along a direction perpendicular to the diffusion front. On the basis of scanning electron microscopy investigations, comparisons are made between the modifications of the polymer network from a sample region rich in one component to the complementary region rich in the other. Such a preparation offers the opportunity to visualize the morphological transformations when a phase transition occurs and the morphologies intrinsic to textures intermediate between well-classified mesomorphic textures. Scanning electron microscopy texture observations are made in parallel with those by optical microscopy in order to make the connection with the mesomorphic textures, which therefore act as indicators during the subsequent SEM investigations.

1. Introduction

The association of a liquid crystal (LC) with a polymer network has opened up a new area of basic and applied research on the behaviour of a LC in a confined geometry. The pioneering work made in the mid-1980s on polymer dispersed liquid crystal (PDLC) systems [1] initiated many investigations devoted to the electro-optics of small droplets of LC in an amorphous polymer matrix [2]. In such composite systems, the polymer concentration is typically in the region of 80 wt %. At the other boundary of the concentration spectrum, investigations started in the 1990s on a new class of LC materials in which the LC is confined in macromolecular and porous networks [3]. In such LC gels, also called polymer stabilized liquid crystals (PSLCs), a small amount of prepolymer—typically a few weight per cent—is dispersed with a photoinitiator in a conventional non-reactive low molar mass LC (LMMLC). A polymer architecture or network is then created *in situ* by UV photocrosslinking. From a fundamental point of view, PSLC may give the opportunity of freezing the molecular order present in the LMMLC. Further subsequent characterizations of the specimen are therefore made possible. As an example, blue phases may be stored in a crosslinked diacrylate film and studied without any temperature control [4]. From a mixture containing only 10 wt % of network-forming chiral material, it is possible to store durably the electric field-induced spiral-shaped patterns from the fingerprint texture of a long pitch cholesteric after the field has been cut off and the fluid LC component removed [5]. For applied research, PSLCs present unique optical and electro-optical properties adapted to applications, e.g. privacy windows, large flexible displays, light shutters for optical signal processing, bistable reflective displays, etc. [3]. With respect to LMMLC cells, PSLC cells may improve stability against mechanical stress in ferroelectric liquid crystal (FLC) displays [6]. The photocrosslinking of a chiral prepolymer in a FLC may also prevent instabilities from nucleating and growing in a sample subjected to an electric field exhibiting some asymmetric features [7].

The nature of the phase separation and the microstructure of the polymer have a crucial influence on the physical properties of the composite material, and may strongly modify the optical and electro-optical behaviours: Bragg reflections for a cholesteric LC with a planar texture, light scattering for a focal-conic texture and a transparent state for a homeotropic texture consequent upon field-induced helix unwinding. In this area, scanning electron microscopy (SEM) gives the opportunity of visualizing the polymer network microstructures. The effect of flexible spacers in the mesogenic monomers and of the temperature of polymerization [8, 9], of the UV

*Author for correspondence

mitov@cemes.fr

curing conditions [10, 11], of the polymer concentration [11–13], or of cell glass surface conditions [14] have been investigated with respect to morphology modifications. Most SEM studies reported to date deal with the final polymer morphology for discrete concentration values.

The aim of this study is to gain knowledge of the polymer architecture created in a new sample geometry when a concentration gradient occurs. A contact preparation between a cholesteric network-forming material and a standard nematic LC is made. In such a sample, the concentration and the anisotropy progressively and homogeneously vary in a direction perpendicular to the diffusion front. In the past, contact preparations have been used to determine by optical methods the helical handedness of a chiral nematic compound relative to a standard material [15], to visualize the rotations of the helical axis due to a concentration gradient [16], in contrast with the wedge-shaped cell used in the Cano method [17], or for diffusion coefficient determinations [18]. Here, studies are focused on the continuous modifications of the polymer network on passing from a sample region rich in one component to the complementary region rich in the other component. Besides, such a sample offers the opportunity of visualizing the morphological transformations when a phase transition occurs and morphologies intrinsic to textures intermediate between well-classified mesomorphic textures. SEM observations are made in parallel with optical microscopy in order to make the connection with mesomorphic textures exhibited by the LC gel, which therefore act like indicators during the subsequent SEM investigations.

2. Experimental

2.1. *Materials*

The UV photocrosslinkable material, RM9, is a cholesteric LC which exhibits selective reflection in the visible spectrum. The mean reflection wavelength of the cured material at normal incidence is 500 nm (with a bandwidth between 50 and 100 nm) when the crosslinking temperature is 80°C. RM9 consists of a mixture of reactive monomers and LC side group polymers with a siloxane backbone. A photoinitiator (Irgacure 651) is added for the UV photocrosslinking purpose. The glass transition temperature of the non-photocrosslinked material is about −10°C and the clearing point is 106°C. Consequently, when mixed with a nematic LC, RM9 simultaneously acts as a chiral mesomorphic dopant and the network-forming substance. The conventional LC is the nematic cyanobiphenyl LC mixture E7 with the following polymorphism: Cr/−10°C/N/60·5°C/I.

2.2. *Sample preparation*

Figure 1 represents the geometry of the preparation. A mixture of RM9 with 2 wt % of photoinitiator is made at 75°C. A drop of this material is spread out on a glass plate on a heating stage in the cholesteric phase at 75°C; a glass cover plate is then put on the material. No surface treatment is used. The sandwich cell is cooled down to 55°C; the LC is then placed in its nematic phase (55°C) at the extremity of the cover plate. It diffuses by capillarity into the empty space of the sandwich cell and makes contact with the RM9 film. The cell gap is about 15 μm and has been subsequently measured by a SEM cross section view. Diffusion is allowed to occur during 20 h. The contact preparation

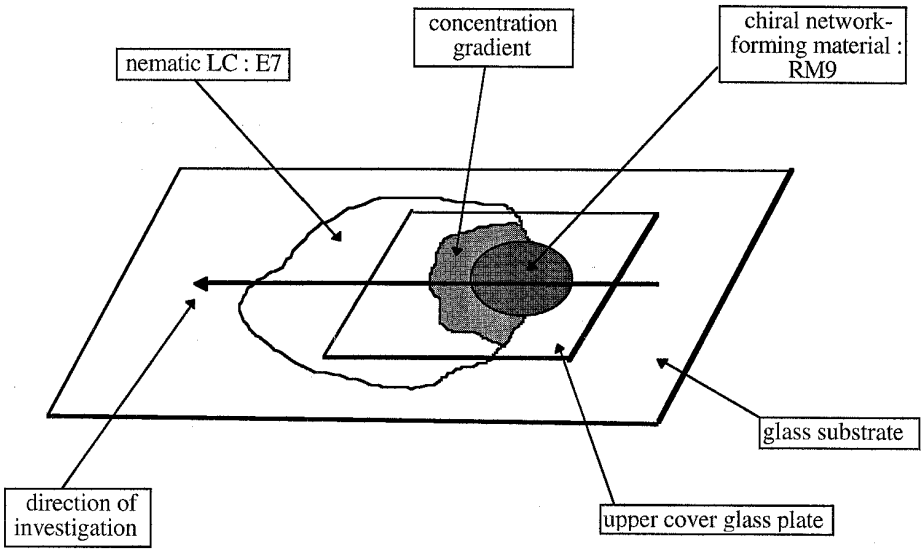

Figure 1. Geometry of the contact preparation.

is then photopolymerized at 55°C with a UV-light curing system (ELC-403 from Electro-Lite Corporation) emitting at 365 nm with a power of 40 mW cm^{-2}, measured with a UV intensity meter (ELC-365); the cell is irradiated for 2 min, i.e. 1 min for each side of the cell. The cell is kept at 55°C during several hours to allow an eventual thermal polymerization to continue. The cell is then plunged into liquid nitrogen (i.e. at a temperature below the glass transition of the polymer) in order to separate the two plates while minimizing plastic distortions of the polymer network. One plate is chosen and immersed in ethanol for several days to dissolve out the

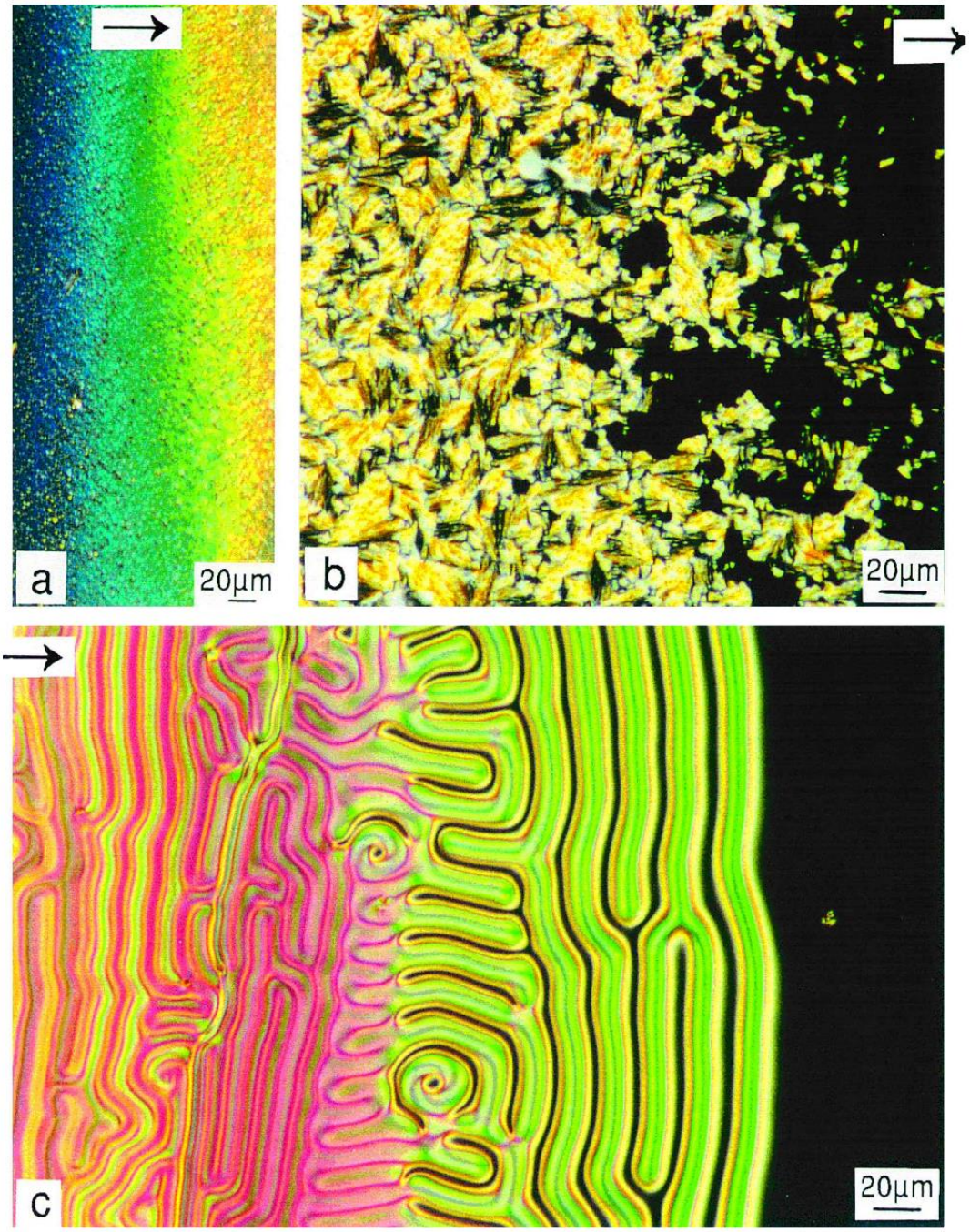

Figure 2. Textures of the contact preparation observed by polarized light microscopy between crossed polarizers before polymerization: (*a*) Bragg cholesteric reflections; (*b*) fan-like (left part) and homeotropic (right part) smectic A textures; (*c*) large pitch cholesteric fingerprint texture and confinement-induced nematic homeotropic texture (black right part). The arrows represent the direction of the investigation (as in figure 1).

fluid LC component and to leave the bare network architecture. This plate is left to dry in an oven at 40°C for a few hours. Once evaporation is complete, the plate is sputtered with a thin layer of gold for SEM study.

2.3. *Morphology examination*

The contact cell was observed at room temperature by optical microscopy between crossed polarizers. Regions are located at every step of the previously described sample preparation. Observations were made before the LC component was removed from the gel; the homeotropic alignment is present when the cell appears dark and an in-plane alignment is present when the sample appears alternately dark and bright while the stage of the microscope is turned. The morphology of the bare network was then observed using a Cambridge 250 SEM operated at 20 kV in the secondary electron imaging mode. Observations were made in the neighbourhood of the surface previously in contact with the cover glass slide.

3. Results and discussion

3.1. *Observations by polarized light microscopy*

In order to establish changes in optical characteristics, the sample was observed by polarized light microscopy before and after polymerization, with the LMMLC component still in place. Figure 2 shows the textures of three main different regions in the contact preparation between crossed polarizers before polymerization at room temperature. The arrows represent the direction referred to in the description. Observations made after polymerization showed that these textures are not altered or modified by the phase separation process brought about by network formation. From the pure RM9 component to pure E7, the distinguishable mesomorphic textures are the following:

(1) Grandjean cholesteric textures exhibiting Bragg reflections in the blue (pure RM9 film) and then green, yellow and orange [figure 2 (*a*)]. These last colours are due to the diffusion of the cholesteric prepolymer into the nematic LC which starts in this region. This results in a cholesteric texture with an increasing pitch.

(2) A fan-shaped texture [left part of figure 2 (*b*)] assigned to the smectic A texture based upon the typical features often described in the literature [19–21] and our previous studies on the miscibility and phase diagrams of mixtures of a cholesteric polysiloxane (related to RM9) and cyanobiphenyl LCs [22, 23].

(3) A homeotropic smectic A texture [black area, right part of figure 2 (*b*)].

(4) A fingerprint cholesteric texture [figure 2 (*c*)]. The line periodicity, related to the half pitch, increases with the concentration in the nematic LC as a consequence of a continuous dilution of RM9 [from the left to the right part of figure 2 (*c*)].

(5) When the helicoidal pitch is similar to the cell gap, a region corresponding to a frustrated cholesteric state is present due to topological incompatibility between the development of the helicoidal structure and the cell gap available for this purpose. In such a region, twisted filaments coexist with a homeotropic texture [black part in figure 2 (*c*)]. When the pitch becomes greater than the cell gap, the texture tends to be homeotropic. In this last region, the chiral polymer is always present, but a confinement-induced helix untwisting arises and prevents detection of its presence by simple optical texture examination. Filament textures and their evolution are consistent with features that have often been described in studies devoted to cholesteric confined systems [24–29].

(6) The typical schlieren texture of E7 nematic LC (not shown on the figure) [19, 21]; the corresponding region is free from RM9.

(7) The intermediate zones between all these well-known mesomorphic textures present no clearly defined textures or perhaps areas of rather abrupt transitions. These zones will not be considered in the present study.

In terms of director orientation, and generally speaking, observations have therefore been described in terms of changes from planar textures to homeotropic textures as a consequence of increasing concentration of cyano molecules whose spontaneous orientation towards a glass plate is known to be homeotropic [30].

3.2. *SEM investigations*

As in the previous section, investigations start from the pure RM9 polymer film towards regions which are rich in LC before its removal and along a line perpendicular to the diffusion front. The sequence of SEM morphologies is presented in figure 3.

The pure RM9 polymer film exhibits a very dense and compact texture without specific structures, except for holes or distortions [figure 3 (*a*)]. They may be due to the presence of air bubbles during the fabrication of the sandwich cell and to modifications brought about by the plate separation process; this polymer-rich phase probably exhibits some rigidity in which deformations may occur.

Immediately after, a texture exhibiting a dense network of fused fibres aligning in the plane of the plate is

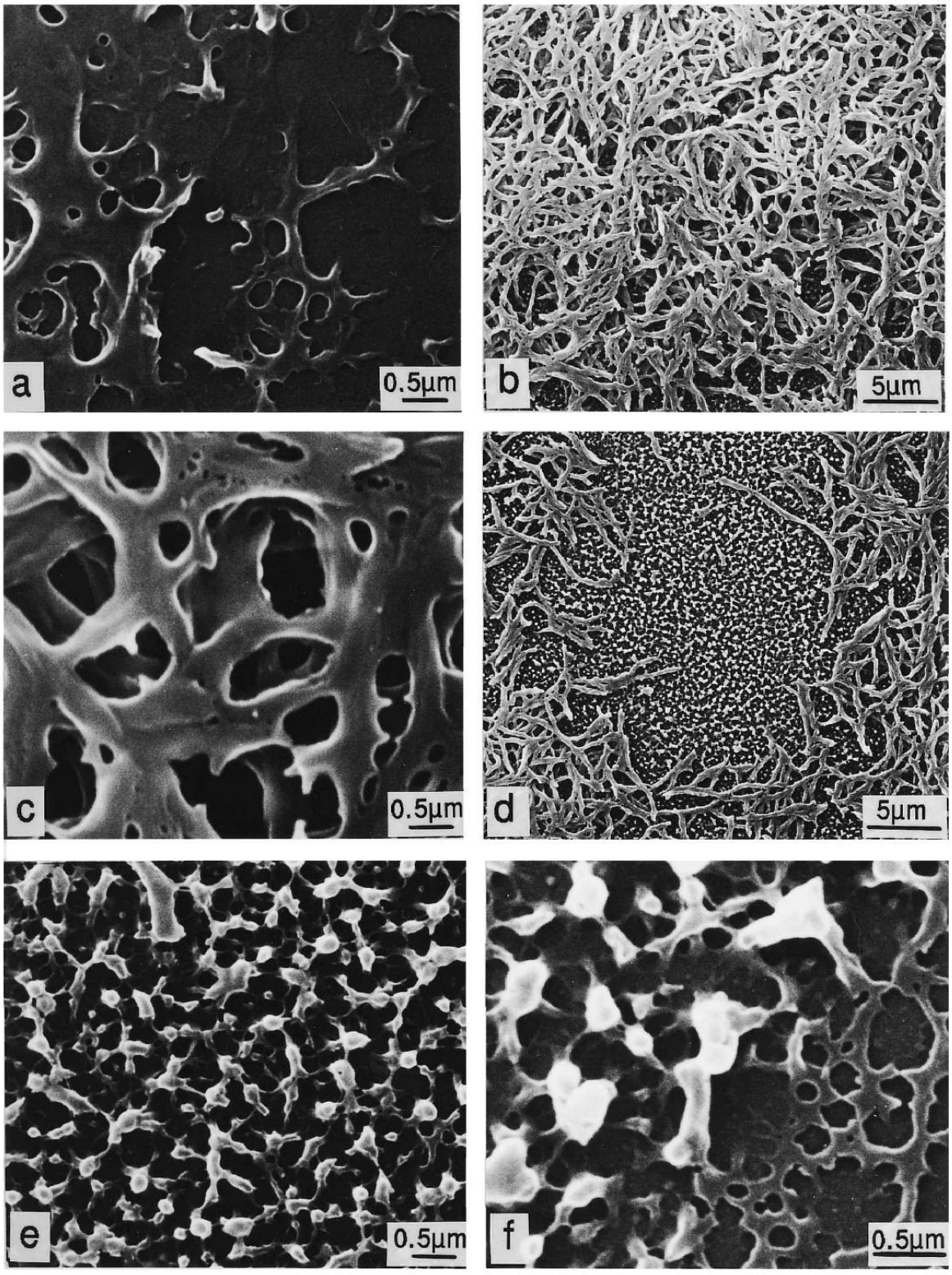

Figure 3. SEM micrographs of the polymer network. Investigations are made from polymer-rich to polymer-poor regions: (*a*) cholesteric polymer film; (*b*) fibre network related to the fan-like smectic A texture; (*c*) magnified view of region shown in (*b*), (*d*) coexistence of polymer fibre and ball patterns, respectively, related to the fan-like and homeotropic smectic A textures; (*e*) magnified view of ball patterns; (*f*) transition region between ball patterns and a porous network related to the frustrated cholesteric region; (*g*)–(*j*) evolution of the porous network when the concentration of network-forming material progressively decreases. Magnified views are inserted for these last four pictures (bar scale=0·5 µm).

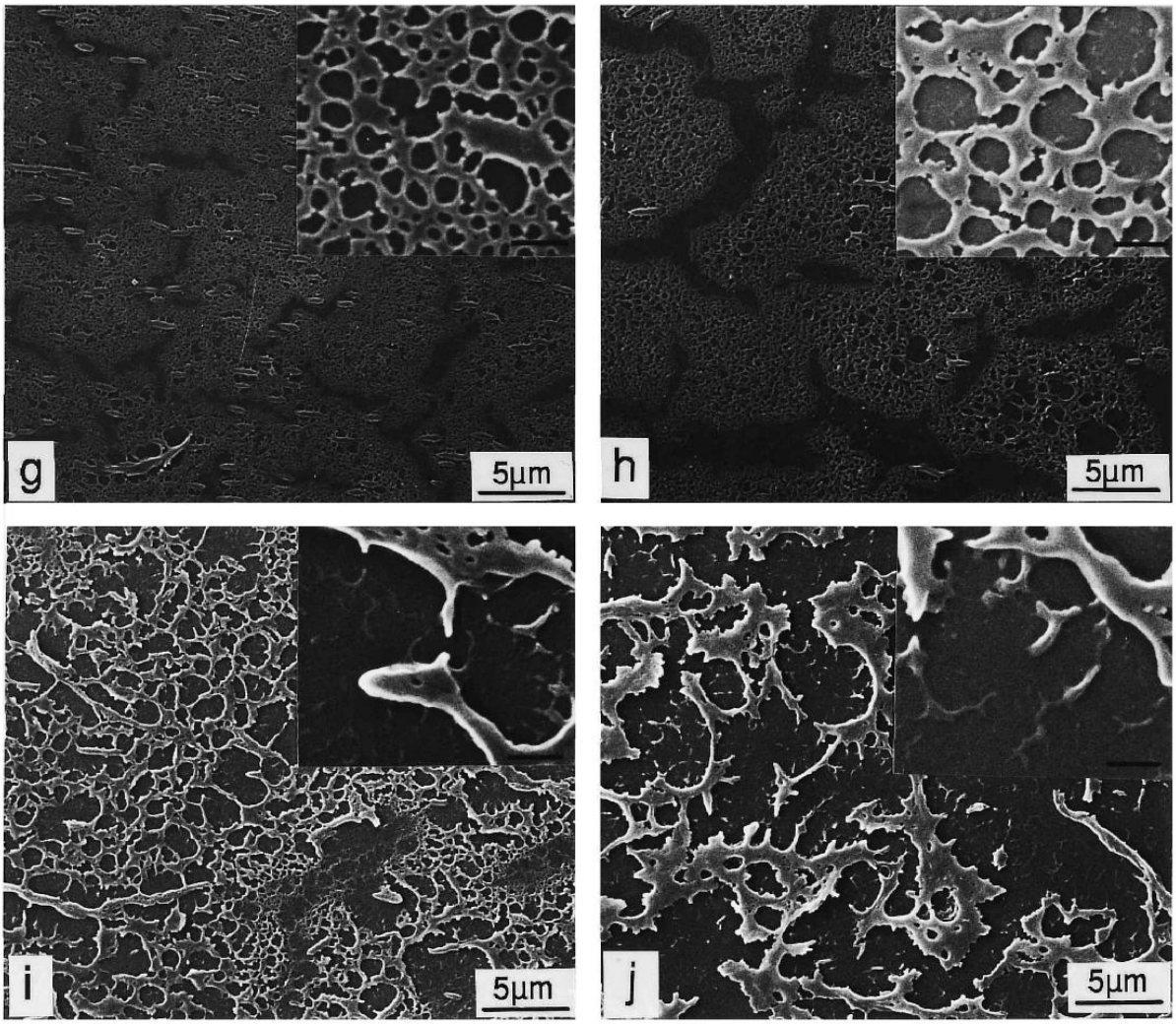

Figure 3. (*Cont.*)

encountered [figure 3 (*b*) and (*c*)]. These fibres form a network with pores of varying size, shape and orientation. The fibre width varies between 0·2 and 0·4 μm. This region corresponds to the fan-like smectic A texture seen by optical microscopy. The polymer network patterns are therefore parallel to the surface and it is striking to see how they mimic the configuration of the LC director. These structures are very similar to the fibres exhibited by planar textures in different mixtures, also containing cyanobiphenyls, and corresponding either to the cholesteric phase [14] or equally to the smectic A phase [9]. Such fibrillar structures are very important in polymer stabilized cholesteric LC texture displays; their size may affect the stability of the display and the density controls the focal-conic domain size [14]. When observations are directed towards regions corresponding only to the smectic A phase, but this time where fan domains coexist with homeotropic areas, the SEM texture reveals fibres coexisting with a porous net exhibiting polymer balls [figure 3 (*d*) and (*e*)]. The ball diameter varies between 0·1 and 0·3 μm. This scale is consistent with the scale corresponding to the fibre width.

The polymer ball pattern becomes predominant when movement across the sample continues, and appears to be the consequence of the polymerization in the homeotropic smectic A phase of the mixture. This feature suggests that the homeotropic orientation of the network has favoured the departure of the LC component when the sample was immersed in alcohol, and this is not surprising if we consider that this texture corresponds to structures perpendicular to the surfaces. The sequence shown in figure 4, designed to reveal what happens in the third direction, yields information about this hypothesis. A region simultaneously exhibiting fibre and ball patterns has been chosen. The sample surface is progressively tilted around a defined axis contained in the surface plane from 0 to 80°. The rotation axis is along the long side of the pictures. It becomes more and more evident

Accepted version published in: *Liquid Crystals*, **23**, 903-910 (1997)

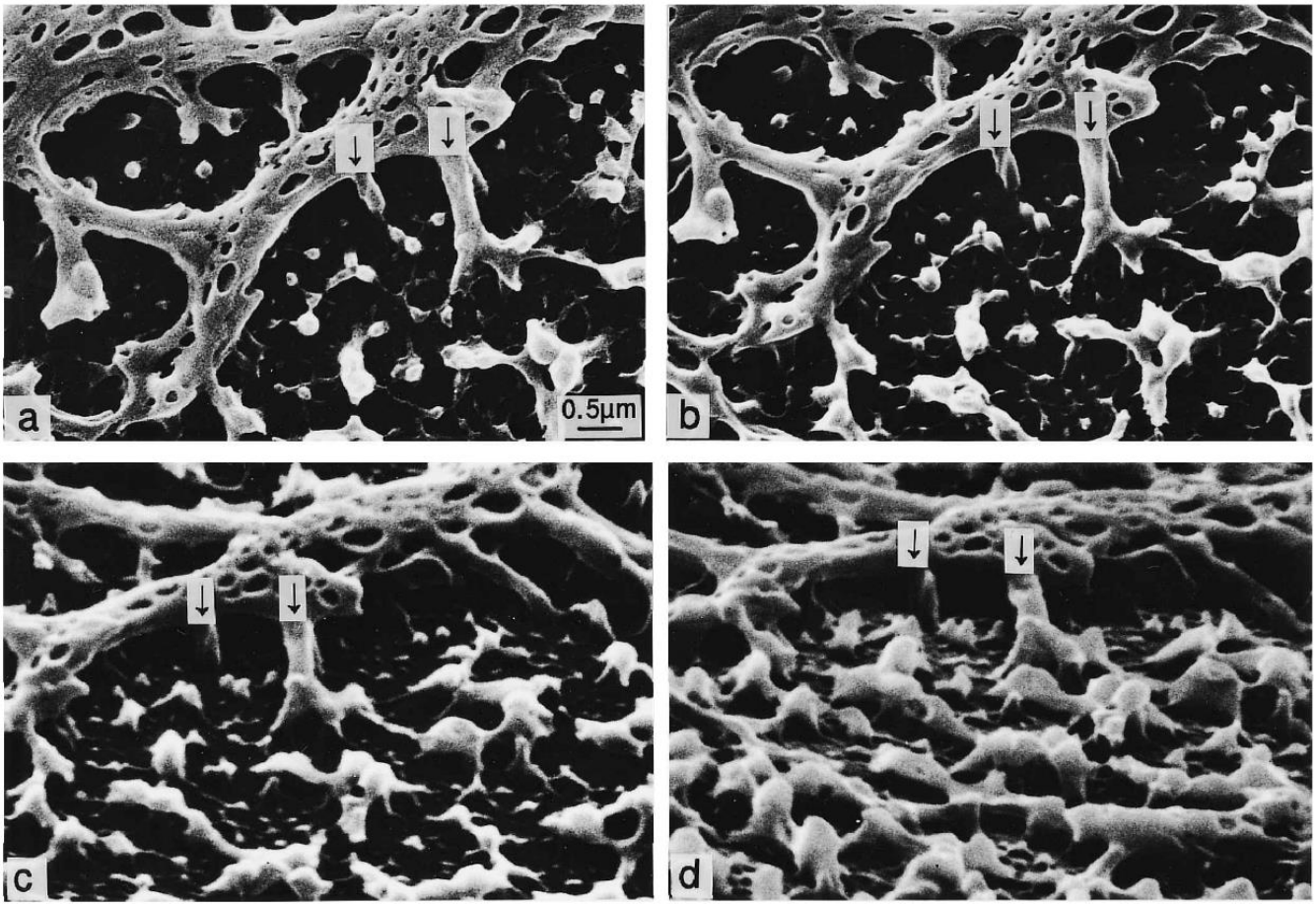

Figure 4. SEM micrographs of the polymer network in a region analogous to region (*d*) of figure 3 (fibres coexisting with balls) when the sample surface is progressively tilted around a defined axis. The rotation axis is along the long side of the pictures; investigations are made for different values of the tilt angle. The arrows are guides for the eye from one picture to the other: (*a*) 0°, (*b*) 30°, (*c*) 60°, (*d*) 80°.

during the rotation that the ball patterns appear to be dome-like patterns with the long axis perpendicular to the sample surface. Such observations reinforce the conclusion that the polymer morphology mimics the director configuration intrinsic to the phase in which polymerization occurs. The polymer morphology reflects its molecular orientation.

The polymer ball pattern remains when the cholesteric phase with an evolving large pitch is encountered. The investigations having been made in the neighbourhood of the upper plate, this fact suggests that the absence of a drastic modification of morphology is due to the constant orientation of the director, maintained homeotropic, although the bulk mesomorphic order evolves from a non-helicoidal structure (homeotropic smectic A phase) to a helicoidal one (cholesteric phase with the helicoidal axis parallel to the surface).

Figure 3(*f*) permits continuous visualization of the network morphology transformation when unwinding of the surface-induced cholesteric helix occurs in the preparation. It can be seen at a distance of about a quarter of a micron that the polymer balls occur together with the next polymer architecture, which consists of an arborescent network with large pores. Such an event must be especially dependent on the prepolymer concentration, the rate of polymerization and the LMMLC viscosity, parameters affecting the anisotropic diffusion. The porous network [right part of figure 3(*f*)] is related to regions corresponding to a frustrated cholesteric state, when the pitch is greater than the cell gap. This porous network becomes less continuous or coherent as the concentration of LC becomes greater. From figure 3(*g*) to 3(*j*), the evolution of gaps in the arborescent network pattern suggests that we treat this sequence as a percolated system in which more and more bonds are cut. Simultaneously, the phase separation in this polymer-poor region involves a network shrinkage due to rejection of the LMMLC solvent in association with the topology of a frustrated cholesteric phase. Also, this fragile architecture may have been exposed to aggregation when

the plate was immersed in alcohol; the polymer network may collapse and there may be some residual LC on the polymer network surface. These factors, added to the overall fact that the network has to be coated with gold, may also cause a discrepancy between the real size and the observed size of microstructures observed under SEM.

The strength of the orientational coupling between network and LC depends on the orientational order of the mixture prior to photopolymerization and the morphological features of the polymer network which is formed. These two parameters are of mutual influence, since the molecular orientation acts on the type of phase separation which in turn affects the orientational order in the medium.

4. Conclusion

Polymer microstructures are very important in polymer stabilized cholesteric LC texture displays since the nature of the phase separation and microstructures of the polymer have a crucial influence on the physical properties of the composite material and may strongly modify the optical and electro-optical behaviours. A contact preparation has been made between a cholesteric photocrosslinkable material and a standard nematic liquid crystal. The concentration and the anisotropy progressively and homogeneously vary along a direction perpendicular to the diffusion front. On the basis of SEM investigations, attention has been focused on the modifications of the polymer network morphology. Samples were first observed intact by polarized-light microscopy before and after polymerization, with the LMMLC component still in place. From the polymer-rich regions to the polymer-poor regions, the distinguishable mesomorphic textures are: Grandjean cholesteric, fan-shaped and homeotropic smectic A, fingerprint cholesteric, with an increasing periodicity until a confinement-induced nematic phase occurs. Two main types of patterns are seen: fibres and balls, respectively, related to fan-shaped and homeotropic smectic A or cholesteric fingerprint textures. These patterns may coexist and are intimately linked, as tilting of the sample has stressed. Moreover, it has been shown that the network mimics the configuration of the LC director, since fibres align in the plane of the substrate and patterns appearing like balls at normal incidence are in fact seen to be homeotropic dome-like patterns when the viewing angle varies. A porous network is related to regions corresponding to the frustrated cholesteric state, when the pitch is greater than the cell gap. This porous network becomes less continuous or coherent as the concentration of the LC becomes greater.

We thank Dr F.-H. Kreuzer for the photocrosslinkable compound.

References

[1] Doane, J. W., Vaz, N., Wu, B.-G., and Zumer, S., 1986, *Appl. Phys. Lett.*, **48**, 269.
[2] Kitzerow, H. S., 1994, *Liq. Cryst.*, **16**, 1.
[3] *Liquid Crystals in Complex Geometries*, 1996, edited by G. P. Crawford and S. Zumer (London: Taylor and Francis).
[4] Kitzerow, H. S., Schmid, H., Ranft, A., Heppke, G., Hikmet, R. A. M., and Lub, J., 1993, *Liq. Cryst.*, **14**, 911.
[5] Mitov, M., and Sixou, P., 1995, *J. mater. Sci. Lett.*, **14**, 1518.
[6] Pirs, J., Blinc, R., Marin, B., Pirs, S., and Doane, J. W., 1995, *Mol. Cryst. Liq. Cryst.*, **264**, 155.
[7] Mitov, M., Ishii, H., Andersson, G., Komitov, L., Lagerwall, S. T., and Sixou, P., 16th International Liquid Crystal Conference, 1996, Kent State University, Kent (Ohio, USA), session D1, P.53.
[8] Rajaram, C. V., Hudson, S. D., and Chien, L. C., 1995, *Chem. Mater.*, **7**, 2300.
[9] Muzic, D. S., Rajaram, C. V., Chien, L. C., and Hudson, S. D., 1996, *Pol. adv. Techn.*, **7**, 737.
[10] Yamaguchi, R., Sudo, N., and Sato, S., 1994, *Techn. Report of IEICE*, **62**, 1.
[11] Chang, S. J., Lin, C. M., and Fuh, A. Y. G., 1996, *Liq. Cryst.*, **21**, 19.
[12] Park, K., Kikuchi, H., and Kajiyama, T., 1994, *Polym. J.*, **26**, 895.
[13] Guymon, C. A., Hoggan, E. N., Walba, D. M., Clark, N. A., and Bowman, C. N., 1995, *Liq. Cryst.*, **19**, 719.
[14] Yang, D. K., Chien, L. C., and Fung, Y. K., 1996, *Liquid Crystals in Complex Geometries*, edited by G.P. Crawford and S. Zumer (London: Taylor and Francis) p. 103.
[15] Goodby, J. W., 1991, *J. mater. Chem.*, **1**, 307.
[16] Kelker, H., 1972, *Mol. Cryst. liq. Cryst.*, **15**, 347.
[17] Cano, R., 1967, *Bull. Soc. Fr. Minér. Cristallogr.*, **90**, 333.
[18] Hakemi, H., and Labes, M. M., 1975, *J. chem. Phys.*, **63**, 3708.
[19] Demus, D., Diele, S., Grande, S., and Sackmann, H., 1983, in *Advances in Liquid Crystals*, Vol. 6, edited by Glenn H. Brown (Academic Press) p. 1.
[20] Prost, J., 1984, *Adv. Phys.*, **33**, 1.
[21] Noel, C., 1989, in *Side-Chain Liquid Crystal Polymers*, edited by C. B. McArdle (Glasgow: Blackie) p. 159.
[22] (*a*) Mitov, M., and Sixou, P., 1992, *J. Phys. II*, **2**, 1659; (*b*) Mitov, M., 1993, PhD thesis, Université de Nice-Sophia Antipolis.
[23] Mitov, M., and Sixou, P., 1993, *Mol. Cryst. liq. Cryst.*, **231**, 11.
[24] Cladis, P. E., and Kleman, M., 1972, *Mol. Cryst. liq. Cryst.*, **16**, 1.
[25] Brehm, M., Finkelmann, H., and Stegemeyer, H., 1974, *Ber. Bunsenges. phys. Chem.*, **78**, 883.
[26] Haas, W., and Adams, J., 1974, *Appl. Phys. Lett.*, **25**, 535.
[27] Press, M. J., and Arrott, A. S., 1976, *J. Phys.*, **37**, 387.
[28] Harvey, T., 1978, *Mol. Cryst. liq. Cryst.*, **34**, 224.
[29] Pirkl, S., 1991, *Cryst. Res. Technol.*, **26**, K111.
[30] Lavrentovich, O. D., Nazarenko, V. G., Pergamenshchik, V. M., Sergan, V. V., and Sorokin, V. M., 1991, *Sov. Phys. JETP*, **72**, 431.